Table 2. Laboratory data obtained upon admission for the treatment of pericardial effusion

Coagulation		**Tumor marker**	
Prothrombin time (INR)	1.08	Carcinoembryonic antigen	0.8 ng/ml
APTT	79 s	Carbohydrate antigen 19-9	80 ng/ml
Endocrine function tests		**Autoimmunity**	
Brain natriuretic peptide	558.5 pg/ml	CH50	47 U/ml
Thyroid-stimulating hormone	0.56 μU/ml	C3c	117 mg/dl
Free triiodothyronin	1.76 ng/ml	C4	22.3 mg/dl
Free thyroxin	1.15 ng/ml	Antinuclear antibody	<40 mg/dl
		Anti-DNA antibody	—
		Anti-Sm antibody	—
		Rheumatoid factor	160-fold
		Proteinase-3-ANCA[d]	<1.3 U/ml
		Myeloperoxidase ANCA[d]	<1.3 U/ml

INR, international normalized ratio; APTT, activated partial thromboplastin time; CH50, 50% hemolytic unit of complement; ANCA, anti-neutrophil cytoplasmic antibody.

Table 3. Virological examination of blood samples (neutralizing antibody titer)

	Acute phase at the time of admission (Oct 2009)	Convalescence phase 4 weeks after the acute phase (Dec 2009)
Adenovirus type7	Negative	Negative
Echovirus type6	Negative	Negative
Echovirus type9	Negative	Negative
Coxsackie B1	4-fold	Negative
Coxsackie B2	16-fold	16-fold
Coxsackie B3	16-fold	32-fold
Coxsackie B4	32-fold	32-fold
Coxsackie B5	4-fold	8-fold
Rapid influenza diagnostic test		
Influenza A	—	
Influenza B	—	

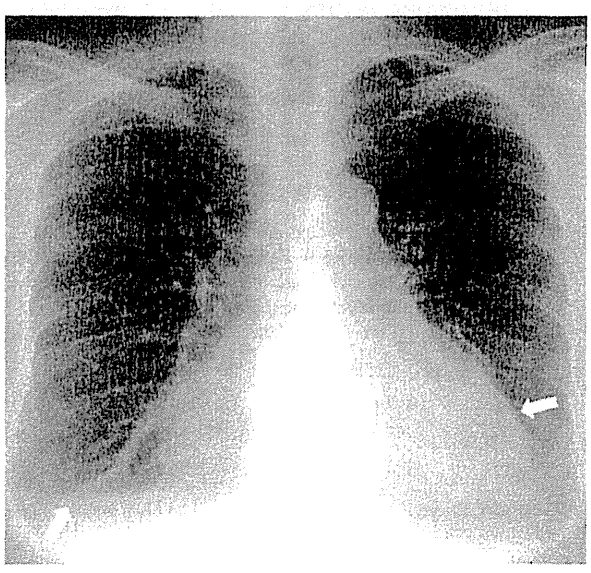

Figure 1. Chest X-ray obtained upon admission shows cardiac enlargement (60%), increased pulmonary markings and bilateral pleural effusion.

observed (Figs 1 and 2). An emergency echocardiography demonstrated a large amount of pericardial effusion (left ventricle: 15 mm) and a slightly pendular left ventricular wall motion. The ejection fraction was 59%. An abdominal CT revealed local recurrence in the remnant stump of the pancreas; the tumor size was slightly decreased when compared with that before the start of gemcitabine therapy. The serum level of CA19-9 had decreased to 31 ng/ml. Pericardiocentesis was immediately performed to prevent the development complication of cardiac tamponade and to examine the cause of the pericardial effusion. An indwelling drain yielded ~700 ml of fluid on the first day, which resulted in the improvement of the patient's hemodynamic condition and marked alleviation of both the exertional dyspnea and the edema; however, no evidence of decrease in the size of the bilateral pleural effusion was noted. Cytology of the pericardial and pleural fluid samples was negative for malignant cells, and both the pericardial and pleural fluid

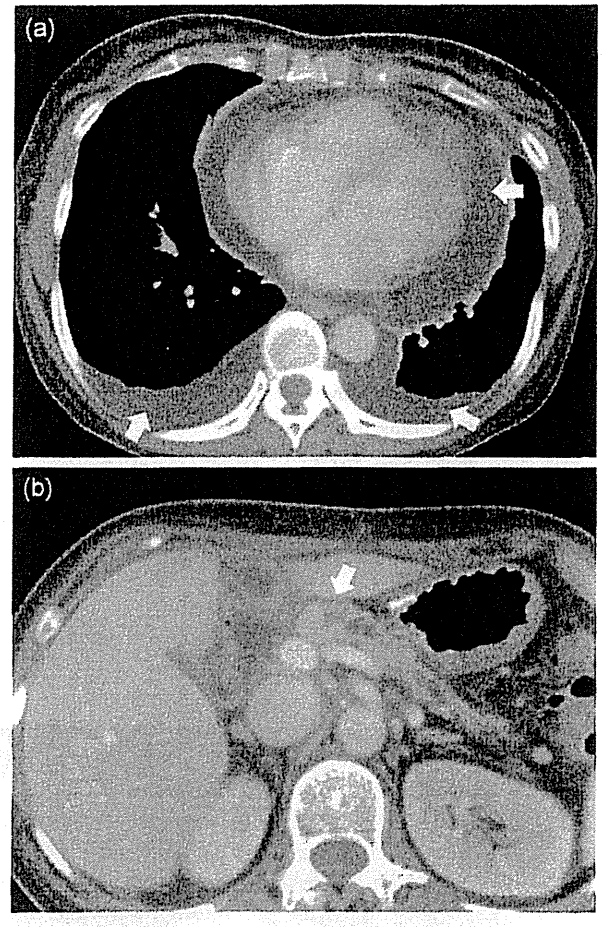

Figure 2. (a) Computed tomographic examination of the chest obtained upon admission shows pericardial effusion and bilateral pleural effusion. (b) Computed tomographic examination of the abdomen obtained upon admission shows local recurrence in the remnant stump of the pancreas; the recurrence was almost the same size as that observed 2 months previously.

Table 4. Laboratory data for effusions obtained upon admission because of pericardial effusion

	Pleural effusion (right)	Pleural effusion (left)	Pericardial effusion
Total protein (g/dl)	2.4	2.4	3.8
LDH (IU/l)	224	237	1796
Glucose (mg/dl)	145	140	55
CEA (ng/ml)	0.3	0.3	3.4
CA19-9 (ng/ml)	11	9	32
Culture	Negative	Negative	Negative
Cytology	No malignant cell	No malignant cell	No malignant cell

LDH, lactate dehydrogenase.

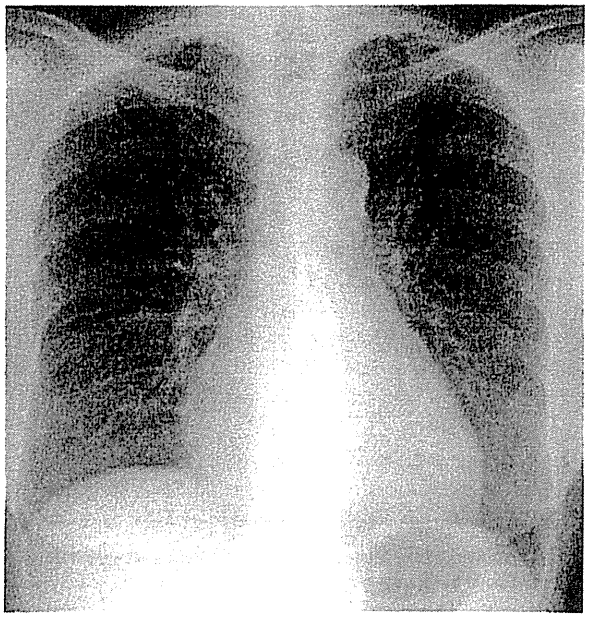

Figure 3. Chest X-ray obtained 2 months after discharge showing a normal cardiac shadow.

samples were clear, pale yellow in color and classified as exudates. The lactate dehydrogenase level of the pericardial aspirate was elevated, and the glucose level was low. Cultures of both the pericardial and pleural fluid specimens for bacteria, mycobacteria and fungi were negative (Table 4). To treat the residual bilateral pleural effusion, the patient was given furosemide 20 mg for 4 days and also a preparation of human serum albumin (8.8 g) for 3 days to counter the possible contribution of hypoalbuminemia, which may cause the pleuropericardial effusion to worsen. Thereafter, the bilateral pleural effusion completely resolved. The daily drainage volume of the pericardial effusion fluid decreased to <100 ml on the 12th day after the pericardiocentesis procedure, and the drainage tube was removed. Echocardiography demonstrated the dramatic decrease in pericardial effusion (left ventricle: <5 mm) and improvement of the ejection fraction to 76%. The patient was discharged from the hospital 20 days after the emergency admission. Two months later, an X-ray of the chest showed a normal cardiac shadow (Fig. 3), and no evidence of pleural/pericardial effusion. In view of the risk of relapse of the pleuropericardial effusions, re-administration of gemcitabine was avoided. Although we proposed other anticancer agents as second-line chemotherapy, she refused any additional anticancer treatment. Therefore, she received only supportive care thereafter and died 4 months later from hepatic metastasis and failure.

DISCUSSION

The main causes of pleuropericardial effusion are infection (viral, pyogenic, tuberculosis, fungal etc.), acute idiopathic,

uremia, neoplasia, myxedema, acute myocardial infarction, post-radiation reactions, drug-induced reactions, collagen vascular disease, inflammatory bowel disease, aortic dissection and trauma.

In our case, a differential diagnosis between malignant effusion and a benign cause of the effusion was essential in view of the diagnosis of cancer recurrence. The fluid samples were found to be exudates, which by itself is not sufficient to rule out the possibility of malignant effusion. However, cytological examinations of the fluid samples revealed no malignant cells. Furthermore, although liver metastasis was diagnosed in our patient after she was discharged from our hospital, she did not have a relapse of the effusion for a long time after the removal of the drainage tube despite the absence of anticancer treatment. Therefore, a malignant effusion was thought to be unlikely. At the time of the diagnosis of pleuropericardial effusion, the patient's oral intake was sufficient and her serum albumin level was 3.5 g/dl. Therefore, hypoalbuminemia did not cause the pleuropericardial effusion. Although proteinuria (2+) and hematuria (3+) were observed at the time of the diagnosis of pleuropericardial effusion, the serum creatinine level was normal. The renal dysfunction may have been caused by hypertension and the chemotherapy. The severity of the renal dysfunction was too low to be a possible cause of the pleuropericardial effusion. Bacteriologic and mycobacteriologic cultures of the blood, pericardial and pleural fluid (both sides) samples were all negative. Complement fixation tests of paired serum samples to detect an elevation in the antibodies to major causative viruses of pleuropericardial effusion were negative. Chest pain, high fever and ST elevation on the electrocardiogram, which are typical findings of acute pericarditis induced by viral infection, were absent. The patient did not have any history of injury, radiation or thoracic surgery. Other causative diseases, such as collagen vascular diseases, cardiovascular diseases, renal failure and hypothyroidism, were excluded based on the results of the physical examination, laboratory examination and imaging studies. Although the use of common medicines was continued, with the discontinuation of gemcitabine, after the diagnosis of the pleuropericardial effusion, the effusion did not recur. In view of the above-mentioned clinical information, we concluded that the most probable cause of the pleuropericardial effusion in our patient was the gemcitabine treatment. Although the re-administration of gemcitabine with follow-up might have improved the reliability of our conclusion, such treatment was not ethically acceptable, especially as the patient refused any further chemotherapy.

Although pulmonary toxicity is a well-known side effect of gemcitabine, there have been only a few reports of pleural effusion developing as a complication secondary to the pulmonary toxicity of this drug (17–20). With regard to pericardial effusion, only one previous report describing four cases of pericardial effusion caused by gemcitabine-induced radiation recall reactions was identified (10). Therefore, our case is the first report of pleuropericardial effusion induced by gemcitabine treatment alone.

The mechanism underlying the development of gemcitabine-induced pleuropericardial effusion is unknown. With regard to reports of pleuropericardial effusion caused by other anticancer agents, this has often been reported in patients treated with docetaxel, dasatinib or imatinib. Docetaxel is a cytotoxic agent that is toxic to the microtubule assembly in the cells. Docetaxel-induced pleuropericardial effusion is reported to be associated with systemic fluid retention caused by the capillary protein leak syndrome (11,12). Although no cases of pleuropericardial effusion have been reported, some cases of gemcitabine-induced systemic capillary leak syndrome have been reported previously (13–15). Favorable effects of corticosteroids, which significantly delay the onset of docetaxel-induced fluid retention, have been reported (16), and this treatment could also be considered for the treatment of gemcitabine-induced pleuropericardial effusion. The colloid osmotic pressure of edema, the interstitial fluid pressure and the interstitial hydrostatic pressure were measured before and after treatment to explain the theory of treatment-induced capillary protein leakage as the mechanism responsible for the fluid retention in patients treated with docetaxel (12). On the other hand, imatinib and dasatinib, molecular-targeted agents categorized as multitargeted tyrosine kinase inhibitors, have been reported to cause pleuropericardial effusion. The underlying mechanism is still unknown, but may involve an immune-mediated pathway or off-target inhibition of the platelet-derived growth factor receptor, β-polypeptide (8). Gemcitabine, a novel deoxycytidine analog antimetabolite, does not exert off-target kinase inhibition.

If the above-mentioned discussions are taken into consideration, the pleuropericardial effusion in our case could have been associated with the capillary leak syndrome induced by gemcitabine.

Complications of pleuropericardial effusion, especially cardiac tamponade, complicating pericardial effusion, and acute respiratory failure complicating pleural effusion are life-threatening and might have a rapid clinical course. Therefore, it should be kept in mind during chemotherapy with gemcitabine, especially when patients complain of dyspnea, tachycardia or edema.

CONCLUSION

We encountered a case of gemcitabine-induced pleuropericardial effusion in a patient with recurrent pancreatic cancer. Physicians should be aware of the possibility of gemcitabine-induced pleuropericardial effusion.

Funding

This work was not supported by any funding sources.

Conflict of interest statement

Takuji Okusaka has received research findings and honoraria from Eli Lilly Japan. Hideki Ueno has received honoraria from Eli Lilly Japan.

References

1. Ohtani Y, Sumi Y, Hisauchi K, et al. Procainamide-induced lupus in a patient with bilateral effusion. *Nihon Kokyuki Gakkai Zassi* 1998;36:535–40.
2. Ghose MK. Pericardial tamponade. A presenting manifestation of procainamide-induced lupus erythematosus. *Am J Med* 1975;58:581–5.
3. Carey RM, Coleman M. Pericardial tamponade: a major presenting manifestation of hydralazine-induced lupus syndrome. *Am J Med* 1973;54:84–7.
4. Bass BH. Hydralazine lung. *Thorax* 1981;36:695–6.
5. Varenika V, Blanc PD. A patient on RIPE therapy presenting with recurrent isoniazid-associated pleural effusions: a case report. *J Med Case Reports* 2011;5:558.
6. Siddiqui MA, Khan IA. Isoniazid-induced lupus erythematosus presenting with cardiac tamponade. *Am J Ther* 2002;9:163–5.
7. Webb DB, Whale RJ. Pleuropericardial effusion associated with minoxidil administration. *Postgrad Med J* 1982;58:319–20.
8. Kelly K, Swords R, Mahalingam D, Padmanabban S, Giles FJ. Serosal inflammation (pleural and pericardial effusions) related to tyrosine kinase inhibitors. *Targ Oncol* 2009;4:99–105.
9. Breccia M, D'elia GM, D'Andrea M, et al. Pleuralpericardic effusion as uncommon complication in CML patients treated with Imatinib. *Eur J Haematol* 2005;74:89–90.
10. Vogl DT, Glatstein E, Carver JR, et al. Gemcitabine-induced pericardial effusion and tamponade after unblocked cardiac irradiation. *Leuk Lymphoma* 2005;46:1313–20.
11. Vincenzi B, Santani D, Frezza AM, Rocci L, Tonini G. Docetaxel induced pericardial effusion. *J Exp Clin Cancer Res* 2007;26:417–20.
12. Semb KA, Aamdal S, Oian P. Capillary protein leak syndrome appears to explain fluid retention in cancer patients who receive docetaxel treatment. *J Clin Oncol* 1998;16:3426–32.
13. De Pas T, Curigliano G, Franceschelli L, et al. Gemcitabine-induced systemic capillary leak syndrome. *Ann Oncol* 2001;12:1651–2.
14. Baron D, Mayo A, Kluger Y. Gemcitabine-induced chronic systemic capillary leak syndrome: a life-threatening disease. *Clin Oncol (R Coll Radiol)* 2006;18:90–1.
15. Biswas S, Nik S, Corrie PG. Severe gemcitabine-induced capillary-leak syndrome mimicking cardiac failure in a patient with advanced pancreatic cancer and high-risk cardiovascular disease. *Clin Oncol (R Coll Radiol)* 2004;16:577–9.
16. Piccart MJ, Klijn J, Paridaens R, Nooil M, et al. Corticosteroids significantly delay the onset of docetaxel-induced fluid retention: final results of a randomized study of the European Organization for Research and Treatment of Cancer Investigational Drug Branch for Breast Cancer. *J Clin Oncol* 1997;15:3149–55.
17. Joerger M, Gunz A, Speich R, et al. Gemcitabine-related pulmonary toxicity. *Swiss Med Wkly* 2002;132:17–20.
18. Belknap SM, Kuzel TM, Yarnold PR. Clinical features and correlates of gemcitabine-associated lung injury. *Cancer* 2006;106:2051–7.
19. Sherrod AM, Brufsky A, Puhalla S. A case of late-onset gemcitabine lung toxicity. *Oncology* 2011;5:171–6.
20. Davidoff S, Shah RD, Arunabh T. Gemcitabine-induced respiratory failure associated with elevated erythrocyte sedimentation rate. *Respir Med* 2006;100:760–3.

nature genetics

Whole-genome sequencing of liver cancers identifies etiological influences on mutation patterns and recurrent mutations in chromatin regulators

Akihiro Fujimoto[1,16], Yasushi Totoki[2,16], Tetsuo Abe[1], Keith A Boroevich[1], Fumie Hosoda[2], Ha Hai Nguyen[1], Masayuki Aoki[1], Naoya Hosono[1], Michiaki Kubo[1], Fuyuki Miya[1], Yasuhito Arai[2], Hiroyuki Takahashi[2], Takuya Shirakihara[2], Masao Nagasaki[3], Tetsuo Shibuya[3], Kaoru Nakano[1], Kumiko Watanabe-Makino[1], Hiroko Tanaka[3], Hiromi Nakamura[2], Jun Kusuda[4], Hidenori Ojima[5], Kazuaki Shimada[6], Takuji Okusaka[7], Masaki Ueno[8], Yoshinobu Shigekawa[8], Yoshiiku Kawakami[9], Koji Arihiro[10], Hideki Ohdan[11], Kunihito Gotoh[12], Osamu Ishikawa[12], Shun-ichi Ariizumi[13], Masakazu Yamamoto[13], Terumasa Yamada[12], Kazuaki Chayama[1,9], Tomoo Kosuge[6], Hiroki Yamaue[8], Naoyuki Kamatani[1], Satoru Miyano[3], Hitoshi Nakagama[5,14], Yusuke Nakamura[1,15], Tatsuhiko Tsunoda[1], Tatsuhiro Shibata[2] & Hidewaki Nakagawa[1]

Hepatocellular carcinoma (HCC) is the third leading cause of cancer-related death worldwide. We sequenced and analyzed the whole genomes of 27 HCCs, 25 of which were associated with hepatitis B or C virus infections, including two sets of multicentric tumors. Although no common somatic mutations were identified in the multicentric tumor pairs, their whole-genome substitution patterns were similar, suggesting that these tumors developed from independent mutations, although their shared etiological backgrounds may have strongly influenced their somatic mutation patterns. Statistical and functional analyses yielded a list of recurrently mutated genes. Multiple chromatin regulators, including *ARID1A*, *ARID1B*, *ARID2*, *MLL* and *MLL3*, were mutated in ~50% of the tumors. Hepatitis B virus genome integration in the *TERT* locus was frequently observed in a high clonal proportion. Our whole-genome sequencing analysis of HCCs identified the influence of etiological background on somatic mutation patterns and subsequent carcinogenesis, as well as recurrent mutations in chromatin regulators in HCCs.

To gain insight into the molecular alterations of virus-associated HCC, we performed whole-genome sequencing (WGS) of 27 HCC tumors from 25 affected individuals, including two sets of multicentric tumors (MCTs) and matched normal lymphocytes (**Supplementary Table 1**). This included 11 hepatitis B virus (HBV)-related HCCs, 14 hepatitis C virus (HCV)-related HCCs and 2 HCCs without HBV or HCV infection (NBNC). Two affected individuals (HC3 and HC7) had two independent synchronous tumors, which were determined to be MCTs, not intrahepatic metastases, on the basis of their clinicopathological features. After PCR duplication removal, we obtained an average of 39.8× (tumor) and 32.7× (lymphocyte) coverage of the genomes by uniquely mapping 50–125 bp reads using paired-end sequencing (**Supplementary Fig. 1**). We identified somatic point mutations and indels with a false positive rate of less than 5% and 10%, respectively (**Supplementary Note**). We detected 4,886–24,147 somatic point mutations per tumor (**Fig. 1a** and **Supplementary Table 2**), and the average number of somatic point mutations at the whole-genome level was 4.2 per megabase. One tumor (HC11), which exhibited an exceptionally large number of somatic mutations (24,147 substitutions with predominant C>T/G>A transition at CpGs and 8,950 indels; **Fig. 1a**), was determined to have a DNA mismatch-repair defect due to a somatic nonsense mutation (encoding p.Glu234*) in *MLH1*. Analysis of the ratio of the depth of coverage identified 294 deleted regions ($\log_2$R ratio ≤ -1) and 20 amplified regions ($\log_2$R ratio ≥ 2) (**Supplementary Table 3** and **Supplementary Note**). Inconsistencies in mapped reads and subsequent PCR validation identified an average

[1]Center for Genomic Medicine, RIKEN, Yokohama, Japan. [2]Division of Cancer Genomics, National Cancer Center Research Institute, Tokyo, Japan. [3]Laboratory of DNA Informatics Analysis, Human Genome Center, Institute of Medical Science, The University of Tokyo, Tokyo, Japan. [4]National Institute of Biomedical Innovation, Ibaraki, Osaka, Japan. [5]Division of Molecular Pathology, National Cancer Center Research Institute, Tokyo, Japan. [6]Hepatobiliary and Pancreatic Surgery Division, National Cancer Center Hospital, Tokyo, Japan. [7]Hepatobiliary and Pancreatic Oncology Division, National Cancer Center Hospital, Tokyo, Japan. [8]Department of Gastroenterological Surgery, Wakayama Medical University, Wakayama, Japan. [9]Department of Medicine & Molecular Science, Hiroshima University School of Medicine, Hiroshima, Japan. [10]Department of Gastroenterological Surgery, Hiroshima University School of Medicine, Hiroshima, Japan. [11]Department of Anatomical Pathology, Hiroshima University School of Medicine, Hiroshima, Japan. [12]Department of Surgery, Osaka Medical Center for Cancer and Cardiovascular Diseases, Osaka, Japan. [13]Department of Gastroenterological Surgery, Tokyo Women's Medical University, Tokyo, Japan. [14]Division of Cancer Development System, National Cancer Center Research Institute, Tokyo, Japan. [15]Laboratory of Molecular Medicine, Human Genome Center, Institute of Medical Science, The University of Tokyo, Tokyo, Japan. [16]These authors contributed equally to this work. Correspondence should be addressed to H. Nakagawa (hidewaki@ims.u-tokyo.ac.jp) or T. Shibata (tashibat@ncc.go.jp).

Received 17 January; accepted 30 April; published online 27 May 2012; doi:10.1038/ng.2291

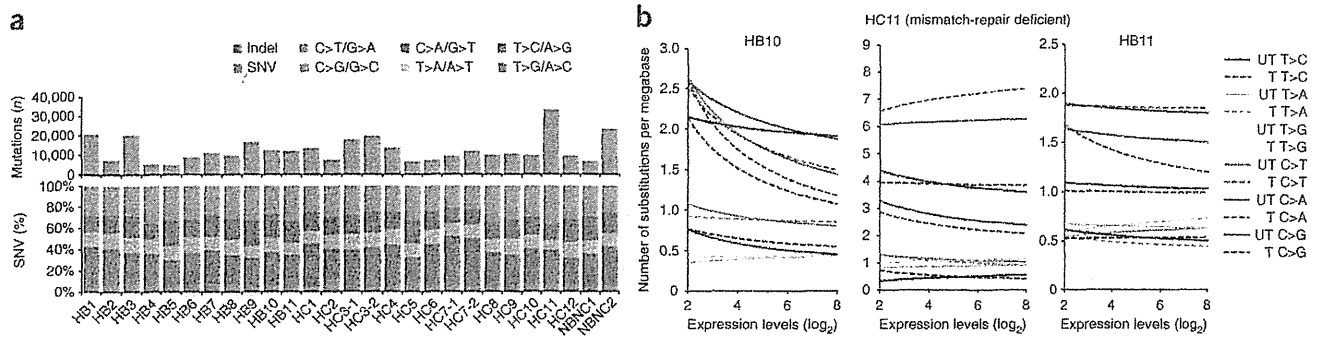

Figure 1 Somatic substitution patterns of HCCs. (**a**) The number of somatic substitutions and indels (top) and somatic substitution patterns (bottom) of the 27 HCC genomes. (**b**) Repair on the transcribed strand. Fitted curves show the effect of gene expression and strand bias on substitution prevalence. We used Agilent microarray expression data (Whole Human Genome 8 × 60K Oligonucleotide Microarray) in this transcription-coupled repair (TCR) analysis, and expression level indicates Agilent microarray intensity level units with a $\log_2$ scale. UT, untranscribed strands; T, transcribed strands.

of 20.8 genomic rearrangements per tumor (**Supplementary Table 4** and **Supplementary Note**). The number of somatic substitutions, indels and rearrangements were not significantly different between HBV- and HCV-related HCCs (**Supplementary Fig. 2**).

The distribution of somatic substitutions in HCC genomes is significantly deviated from the assumption of a uniform mutation rate (χ-square test; P value $< 1 \times 10^{-300}$), and we identified a dominance of T>C/A>G transitions (odds ratio (OR) = 2.02, 95% confidence interval (CI) = 1.95–2.08; **Fig. 1a**), as described previously[1], as well as C>A/G>T transversions (OR = 1.43, 95% CI = 1.36–1.50) and C>T/G>A transitions (OR = 1.75, 95% CI = 1.68–1.82), particularly at CpG sites (OR = 4.55, 95% CI = 4.30–4.80) (**Supplementary Fig. 3**). As C>T/G>A transitions are also dominant in other cancers[2], T>C/A>G transitions and C>A/G>T transversions could be characteristic mutational signatures of HCC genomes.

To examine the influence of transcription-coupled repair, we compared gene expression levels (**Supplementary Tables 5** and **6**) and the number of substitutions in seven HCCs. Only T>C and C>A changes but not C>T changes were effectively repaired on the transcribed strand (**Supplementary Fig. 4a–c**), and these repairs occurred more frequently in highly expressing genes (HB10 in **Fig. 1b** and **Supplementary Fig. 5**). Of note, transcription-coupled repair did not occur in the mismatch repair–deficient tumor with *MLH1* inactivation (HC11 in **Fig. 1b**). Another case (HB11) had a familial disposition to cancer (**Supplementary Table 1**) and exhibited a distinct mutation signature (increased indels, less dominance of T>C/A>G transitions and a decreased effect of transcription-coupled repair at T>C transitions) (**Fig. 1a,b**), although no causal mutation explaining the DNA-repair deficiency was identified. These findings suggest that transcription-coupled repair preferentially repairs somatic substitutions that are specifically increased in cancer.

One of the characteristic features of HCC is multiple occurrences or MCTs in a strong carcinogenetic background. First, we compared somatic mutation sites of the two pairs of MCTs (HC3 and HC7). In protein-coding regions, no common somatic mutations were identified. *ATM*, *FSIP2* and *LRFN5* were mutated in both MCTs of HC3, but the locations of the mutations were different. In non-coding regions, WGS identified 30 and 37 common somatic point mutations and indels in the HC3 and HC7 pairs, respectively. However, most of these occurred in repetitive regions, and all candidates that could be analyzed by Sanger sequencing ($n = 20$) were found to be germline variants (**Supplementary Note**). We also found no common structural alterations in these MCTs (**Fig. 2a**). These findings suggest that these synchronous MCTs developed through an accumulation of a completely different set of genetic alterations. Second, we applied

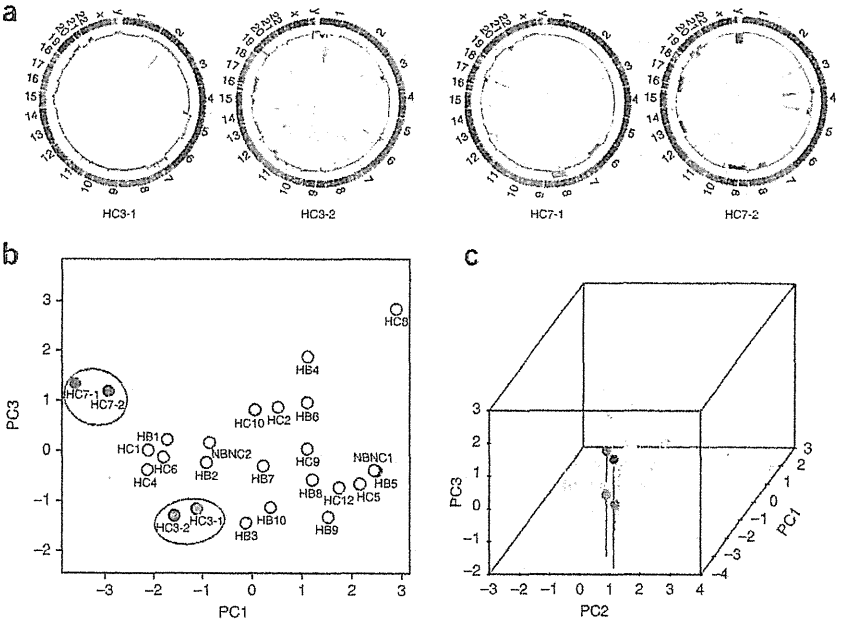

Figure 2 Mutation patterns of MCTs. (**a**) Circos plots[20] of the MCTs from two subjects (HC3 and HC7). Each circle plot represents validated rearrangements (inner arcs) and copy-number alternations (inner rings). In rearrangements, lines show translocations (green), deletions (blue), inversions (orange) and tandem duplications (red). Copy-number gain and loss regions are shown in green and red. (**b**) PCA of the somatic substitution patterns of 25 HCC genomes. Two sets of MCT pairs (HC3 and HC7) are shown by green and blue, respectively, and are circled in red. (**c**) Three-dimensional plot of principal components (PCs) for 25 HCCs on somatic substitution pattern. Two sets of MCT pairs (HC3 and HC7) are shown in green and blue, respectively.

Table 1 Significantly mutated genes and their mutation frequency in the validation set

Gene	Chr.	Start	End	CDS length (bp)	Coding indel	Missense	Nonsense	Splice site	Total	*P* value	*q* value	Frequency in validation set
TP53	17	7,572,927	7,579,912	1,218	0	11	0	3	14	0	0	NA
ERRFI1	1	8,073,270	8,075,679	1,397	1	0	2	0	3	0.00020	0.0034	3.1% (2/65)
ZIC3	X	136,648,851	136,652,229	1,412	0	3	0	0	3	0.00050	0.0041	3.3% (4/120)
CTNNB1	3	41,265,560	41,280,833	2,398	0	3	0	0	3	0.0015	0.0071	NA
GXYLT1	12	42,481,588	42,538,448	1,351	0	3	0	0	3	0.0013	0.0071	0.8% (1/120)
OTOP1	4	4,190,530	4,228,591	1,859	1	2	0	0	3	0.0015	0.0071	0.8% (1/120)
ALB	4	74,270,045	74,286,015	1,882	3	0	0	0	3	0.0022	0.0089	3.3% (4/120)
ATM	11	108,098,352	108,236,235	9,415	1	4	0	0	5	0.0037	0.013	5.0% (6/120)
ZNF226	19	44,674,234	44,681,827	2,424	1	1	1	0	3	0.0043	0.014	3.3% (4/120)
USP25	21	17,102,713	17,250,794	3,260	1	2	0	0	3	0.0051	0.015	0% (0/120)
WWP1	8	87,386,280	87,479,122	2,857	2	1	0	0	3	0.0060	0.016	7.7% (5/65)
IGSF10	3	151,154,477	151,176,497	7,892	0	4	0	0	4	0.0091	0.023	3.3% (4/120)
ARID1A	1	27,022,895	27,107,247	6,934	2	1	0	0	3	0.011	0.026	10% (12/120)
UBR3	2	170,684,018	170,938,353	5,819	0	3	0	0	3	0.018	0.041	0.8% (1/120)
BAZ2B	2	160,176,776	160,335,230	6,643	0	3	0	0	3	0.024	0.050	1.6% (2/120)

Significantly mutated genes with more than two mutations are shown. Chr., chromosome.

principal-component analysis (PCA) to further examine genome-wide somatic mutation patterns. Two HCCs (HC11 and HB11) exhibited quite distinct substitution patterns compared to the other samples due to their mismatch-repair deficiency (**Supplementary Fig. 6a**). Therefore, they were excluded from PCA. Notably, the pairs of each MCT (HC3 and HC7) were tightly clustered in PCA (permutation test; *P* value = 0.00050), indicating similar somatic substitution patterns on the whole-genome level (**Fig. 2b,c**). Considering that these MCTs shared the exact same genetic and environmental backgrounds, the somatic substitution patterns are likely to be determined by the etiological backgrounds in which the tumors developed.

We also examined associations between the principal components and clinical factors. Although the correlations between somatic substitution patterns and age at diagnosis, tumor grade, liver fibrosis and tumor size were not significant, habitual alcohol drinking and the occurrence of synchronous or metachronous multiple liver nodules showed significant association with principal components of the somatic substitution patterns (habitual alcohol drinking, $P = 0.028$; multiple liver nodules, $P = 0.016$) (**Supplementary Fig. 6b,c**). Virus type showed a marginal association with substitution pattern ($P = 0.091$) (**Supplementary Fig. 6d**). In addition to viral infection, alcohol abuse, obesity, diabetes and other metabolic disorders are also risk factors for liver carcinogenesis, and its background etiology is very heterogeneous[3]. Multiple background factors, including germline variants, epigenetic status of liver, virus infection, exposure to other environmental carcinogens, inflammation and a combination of these factors, would contribute to the somatic mutation pattern in cancer genomes.

Across all 27 HCC genomes, we detected a total of 2,048 (75.9 per tumor) protein-altering point mutations, including 1,734 missense mutations, 101 nonsense mutations, 161 short coding indels and 52 splice-site mutations (**Supplementary Table 2**). After adjusting for the regional deviation of somatic mutation rate and gene length, significantly frequent mutations were found to occur in 15 genes, with a false discovery rate (FDR) of ≤0.05 (**Table 1** and **Supplementary Table 7**). *TP53* and *CTNNB1* (encoding β-catenin) genes were significantly mutated in HCC, as previously reported[4]. Five mutations of *ATM* were detected in four tumors without *TP53* mutations. Sequencing analysis on an independent set of 120 HCCs detected 6 additional *ATM* mutations (5%) (**Table 1** and **Supplementary Table 8**). Three mutations of *ARID1A*, two frameshifts and one missense, were detected in three tumors by WGS. *ARID1A* encodes a key component of the SWI-SNF chromatin-remodeling complex, and *ARID1A* mutations have been detected in ovarian cancer[5] and many other cancers[6]. Sequencing analysis of the 120 HCCs detected 12 additional mutations of *ARID1A* (10%) (**Table 1** and **Supplementary Table 8**). WGS detected three somatic mutations in *ERRFI1*, two nonsense and one frameshift, in two tumors. *ERRFI1* encodes a protein that inhibits the kinase domains of EGFR and ERBB2 (ref. 7), and *Errfi1* knockout mice showed enhanced hepatocyte proliferation[8]. These mutations may cause the loss of inhibitory function and thereby activate the EGFR signaling pathway in HCC. We detected 2 additional mutations of *ERRFI1* (3.1%) in 65 independent HCCs (**Table 1** and **Supplementary Table 8**). Three

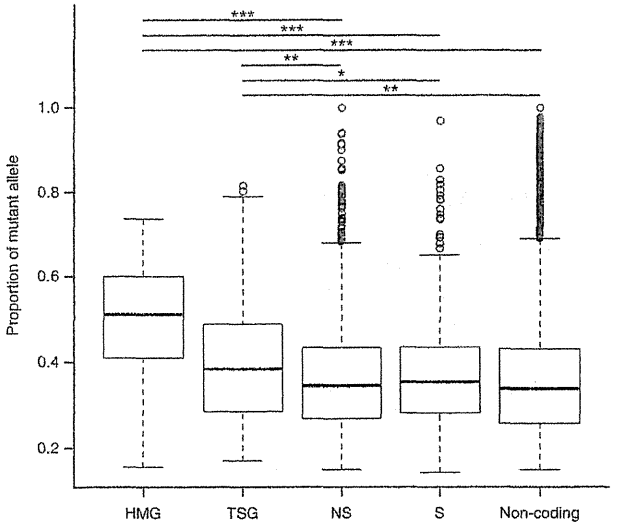

Figure 3 Mutant allele proportions of point mutations. HMG, highly mutated genes, genes whose mutation frequency was greater than 3% in the validation set (*ARID1A*, *IGSF10*, *ATM*, *ZNF226*, *ZIC3*, *WWP1* and *ERRFI1*); TSG, known tumor suppressor genes annotated by MutationAssessor[21]; NS, nonsynonymous; S, synonymous. Non-coding includes point mutations in non-coding regions except for in splice sites. The edges of the boxes represent the 25th and 75th percentile values. The whiskers represent the most extreme data points, which are no more than 1.5 times the interquartile range from the boxes. $^{*}P < 0.05$; $^{**}P < 0.01$; $^{***}P < 0.001$.

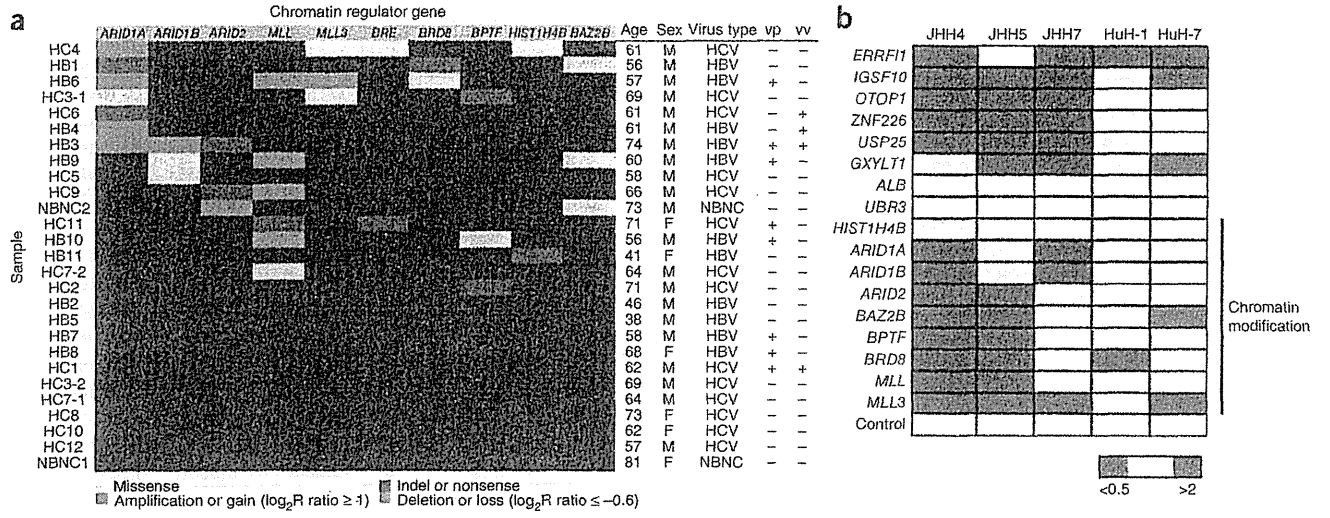

Figure 4 Mutations in chromatin regulators and functional analysis of potential driver genes. (**a**) Mutations in chromatin regulators in 27 HCC genomes. Mutations in chromatin-regulator genes are summarized. In addition to point mutations, 55.6-kb genomic deletion of *ARID2* in NBNC2, which was identified by the read-pair method, and several copy-number alternations of chromatin-regulator genes are included. HC6 had both 1-bp deletion and low-level loss in *ARID1A*. (**b**) Functional assays of potential driver genes in HCC cell lines. Changes in cell proliferation in five HCCs compared to proliferation with control siRNA treatment are presented. Magenta and blue boxes represent more than 2-fold and less than 0.5-fold changes in the cell number, respectively. Genes involved in chromatin modification are indicated by the line.

mutations of *WWP1* were detected by WGS. *WWP1* encodes an E3 ubiquitin ligase that affects protein stability of some oncogenes, such as ERBB4 (ref. 9). We also detected 5 additional mutations (7.7%) of *WWP1* in 65 HCCs (**Table 1** and **Supplementary Table 8**). We detected additional mutations of *IGSF10*, *ZNF226*, *ZIC3* and *ALB*, each at a 3% frequency (**Table 1** and **Supplementary Table 8**), but their functional significance in cancer is unknown. Next, we compared the mutant allele proportions of point mutations in highly mutated genes whose frequency was validated (*ARID1A*, *IGSF10*, *ATM*, *ZNF226*, *ZIC3*, *WWP1* and *ERRFI1*) among the significantly mutated genes, known tumor suppressor genes and non-coding regions. The proportions of point mutation alleles of both highly mutated genes and tumor suppressor genes were significantly higher than that of non-coding regions (**Fig. 3**), which indicates that either the wild-type alleles were deleted or mutations in these genes were generated in the ancestral cell population of tumor cells. The mutant allele proportion or mutation clonality within a tumor would provide useful information to identify driver mutations[10].

To identify biologically relevant mutations in HCCs, we performed gene-set enrichment (GSE) analysis on the mutated genes[11].

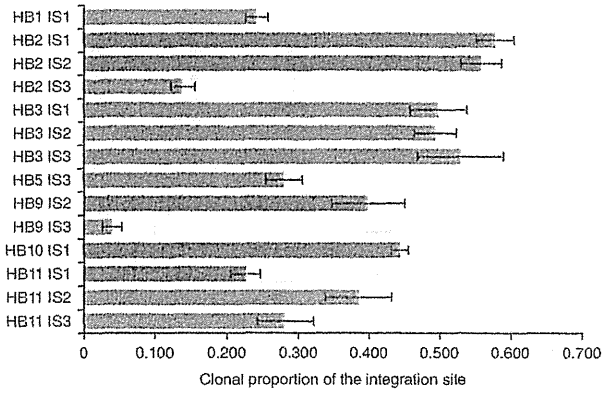

We attempted to enrich functional mutations by selecting genes with deleterious mutations (nonsense, indel and splice-site mutations). In GSE analysis, the 'bromodomain' and 'chromatin-regulator' gene sets were found to be significantly enriched in the mutated gene list (**Supplementary Table 9**). WGS detected recurrent somatic mutations in several genes annotated to be associated with chromatin regulation, such as *ARID1A*, *ARID1B*, *ARID2*, *MLL*, *MLL3*, *BAZ2B*, *BRD8*, *BPTF*, *BRE* and *HIST1H4B*. Notably, 14 out of the 27 tumors (52%) had somatic point mutations or indels in at least one of these chromatin regulators (**Fig. 4a** and **Supplementary Tables 7** and **10**). Sequencing analysis of the 120 independent HCCs detected 8 additional mutations of *ARID1B* (6.7%), 7 of *ARID2* (5.8%), 5 of *MLL3* (4.2%), 2 of *MLL* (1.7%) and 2 of *BPTF* (1.7%), as well as 12 of *ARID1A* (10%) (**Supplementary Tables 8** and **10**). In both the WGS and the validation set, the number of indels was significantly higher in chromatin regulators than in genes in other categories ($P = 2.1 \times 10^{-10}$; indel/nonsynonymous: 23/38 in chromatin regulators and 154/1,820 in genes in other categories), suggesting that loss-of-function mutations are enriched in these chromatin-regulator genes in HCC genomes. We observed that mutations in chromatin regulators were marginally associated with the stage of liver fibrosis and hepatic vein invasion (**Fig. 4a** and **Supplementary Table 11**), supporting the idea that mutations of chromatin regulators or the *ARID* family may contribute to poor prognosis for individuals with HCC.

To determine whether the recurrently mutated genes have any biological affect in HCC, we knocked down 17 candidate driver genes, including the chromatin regulators, through small interfering RNA (siRNA) in a panel of five HCC cell lines (**Supplementary Fig. 7**). Downregulation

Figure 5 Clonal proportion of HBV integration sites in cancer cell populations of four HBV-integrated HCCs. Integration sites (ISs) in the *TERT* locus are indicated by red. Digital PCR analysis indicates 4.0–57.8% clonal population of HBV integration at each locus. The average proportion of the *TERT* integration sites (41%) was higher than that of other integration sites (32%). Error bars, s.e.m. from four replicate measures.

of three genes (*ERRFI1*, *IGSF10* and *MLL3*) promoted cell proliferation in four out of five HCC cell lines when compared to those treated with control siRNA (**Fig. 4b**). Knockdown of another eleven genes promoted cell growth in at least one HCC cell line (**Fig. 4b**). The growth-promoting effect was not observed in HCC cell lines that did not express the gene (**Supplementary Fig. 8**). This data implicates that these candidate driver genes, many of which are chromatin regulators, may have a tumor suppressive effect in HCC cells. The mutated chromatin regulators in HCC may change their target's gene expression though diverse remodeling of nucleosome structures and histone modification[12–14]. Moreover, multiple long non-coding RNAs, suggested to regulate chromatin status and transcription by coupling with chromatin regulators[15], were also mutated at statistically significant frequencies in our WGS analysis (**Supplementary Table 12** and **Supplementary Note**).

We determined HBV integration sites using sequence read-pair mapping information[16]. Twenty-three breakpoints were predicted by 3 or more supporting read-pairs and all were validated by PCR and Sanger sequencing. The breakpoints within the HBV genome were primarily localized to the downstream region of the *HBx* gene whereby deletion of C-terminal region may contribute to development of HCC (**Supplementary Fig. 9**). Interestingly, HBV genome integration was observed within or upstream of the *TERT* gene in four HBV-related HCCs as previously observed[17] (**Supplementary Fig. 10** and **Supplementary Table 13**). Using digital PCR, we quantified the clonal population with HBV integration in seven HBV-integrated HCCs and corresponding non-cancerous liver tissues, and the proportion of the integrated alleles ranged from 4.0% to 57.8% in the tumors (**Fig. 5**), while no clonal integration breakpoint was detected in the paired non-cancerous liver tissues. Considering HBV genome integration is an early event during chronic HBV infection[18], HBV integration in the *TERT* locus may confer clonal advantage in the early phase of HBV-related liver carcinogenesis.

This study provides a comprehensive analysis of the mutational landscape of heterogeneous virus-associated HCC genomes. The variation in somatic substitution patterns in individual tumors may reflect different exposure to carcinogens, DNA repair defects and cellular origin[19]. Considering the high complexity and heterogeneity of HCCs of both etiological and genetic aspects, further molecular classification is required for appropriate diagnosis and therapy in personalized medicine.

URLs. Human Genome Center, The University of Tokyo, http://sc.hgc.jp/shirokane.html; ICGC, http://www.icgc.org/; Gene Expression Omnibus (GEO) database, http://www.ncbi.nlm.nih.gov/geo/; ICGC data portal, http://dcc.icgc.org/; human reference genome (GRCh37), http://www.ncbi.nlm.nih.gov/projects/genome/assembly/grc/human/.

METHODS

Methods and any associated references are available in the online version of the paper.

Accession codes. Information on all point mutations and indels was deposited to the ICGC web site, and the data can be acquired from the ICGC Data Portal site. Microarray expression data are deposited at the Gene Expression Omnibus (GEO) database under the accession number GSE36390.

Note: Supplementary information is available in the online version of the paper.

ACKNOWLEDGMENTS

The supercomputing resource SHIROKANE was provided by the Human Genome Center at The University of Tokyo. The authors thank T. Urushidate, S. Ohashi, N. Okada, A. Kokubu and H. Shimizu at the National Cancer Center Research Institute and C. Inai, R. Ooishi, and R. Kitada at the RIKEN Center for Genomic Medicine for their technical assistances. This work was supported partially by the Program for Promotion of Fundamental Studies in Health Sciences of the National Institute of Biomedical Innovation (NIBIO), the National Cancer Center Research and Development Fund (23-A-8) and the RIKEN Strategic Research Program for R&D of President's Fund 2011.

AUTHOR CONTRIBUTIONS

A.F., Y.T., T.A., K.A.B., F.M., H. Nakamura, T.T., T. Shibata and H. Nakagawa performed data analyses. F.H., Y.A., H. Takahashi, T. Shirakihara, K.N., K.W.-M., T. Shibata and H. Nakagawa performed whole-genome sequencing. F.H., H.H.N., K.N. and K.W.-M. performed the validation sequencing study. F.H., Y.A., H. Takahashi, T. Shirakihara and T. Shibata performed siRNA experiments. A.F., M.A., N.H. and M.K. performed digital PCR and SNP microarray experiments. M.N., T. Shibuya, H. Tanaka and S.M. operated the supercomputer system. H. Ojima, K.S., T.O., M.U., Y.S., Y.K., K.A., H. Ohdan, K.G., O.I., S.A., M.Y., T.Y., K.C., T.K. and H.Y. collected clinical samples. A.F., Y.T., T.T., T. Shibata and H. Nakagawa wrote the manuscript. Y.N., T.T., T. Shibata and H. Nakagawa conceived the study and led the design of the experiments. J.K., N.K., H. Nakagama, Y.N., T. Shibata and H. Nakagawa contributed to the findings for this study.

COMPETING FINANCIAL INTERESTS

The authors declare no competing financial interests.

Published online at http://www.nature.com/doifinder/10.1038/ng.2291.
Reprints and permissions information is available online at http://www.nature.com/reprints/index.html.

1. Totoki, Y. *et al.* High-resolution characterization of a hepatocellular carcinoma genome. *Nat. Genet.* **43**, 464–469 (2011).
2. Greenman, C. *et al.* Patterns of somatic mutation in human cancer genomes. *Nature* **446**, 153–158 (2007).
3. El-Serag, H.B. & Rudolph, K.L. Hepatocellular carcinoma: epidemiology and molecular carcinogenesis. *Gastroenterology* **132**, 2557–2576 (2007).
4. Laurent-Puig, P. & Zucman-Rossi, J. Genetics of hepatocellular tumors. *Oncogene* **25**, 3778–3786 (2006).
5. Wiegand, K.C. *et al. ARID1A* mutations in endometriosis-associated ovarian carcinomas. *N. Engl. J. Med.* **363**, 1532–1543 (2010).
6. Jones, S. *et al.* Somatic mutations in the chromatin remodeling gene *ARID1A* occur in several tumor types. *Hum. Mutat.* **33**, 100–103 (2012).
7. Ferby, I. *et al.* Mig6 is a negative regulator of EGF receptor–mediated skin morphogenesis and tumor formation. *Nat. Med.* **12**, 568–573 (2006).
8. Reschke, M. *et al.* Mitogen-inducible gene–6 is a negative regulator of epidermal growth factor receptor signaling in hepatocytes and human hepatocellular carcinoma. *Hepatology* **51**, 1383–1390 (2010).
9. Li, Y., Zhou, Z., Alimandi, M. & Chen, C. WW domain containing E3 ubiquitin protein ligase 1 targets the full-length ErbB4 for ubiquitin-mediated degradation in breast cancer. *Oncogene* **28**, 2948–2958 (2009).
10. Shah, S.P. *et al.* The clonal and mutational evolution spectrum of primary triple-negative breast cancers. *Nature* published online doi:10.1038/nature10933 (4 April 2012).
11. Huang, W., Sherman, B.T. & Lempicki, R.A. Bioinformatics enrichment tools: paths toward the comprehensive functional analysis of large gene lists. *Nucleic Acids Res.* **37**, 1–13 (2009).
12. Parsons, D.W. *et al.* The genetic landscape of the childhood cancer medulloblastoma. *Science* **331**, 435–439 (2011).
13. Varela, I. *et al.* Exome sequencing identifies frequent mutation of the SWI/SNF complex gene *PBRM1* in renal carcinoma. *Nature* **469**, 539–542 (2011).
14. Lee, J. *et al.* A tumor suppressive coactivator complex of p53 containing ASC-2 and histone H3-lysine-4 methyltransferase MLL3 or its paralogue MLL4. *Proc. Natl. Acad. Sci. USA* **106**, 8513–8518 (2009).
15. Khalil, A.M. *et al.* Many human large intergenic noncoding RNAs associate with chromatin-modifying complexes and affect gene expression. *Proc. Natl. Acad. Sci. USA* **106**, 11667–11672 (2009).
16. Jiang, Z. *et al.* The effects of hepatitis B virus integration into the genomes of hepatocellular carcinoma patients. *Genome Res.* **22**, 593–601 (2012).
17. Paterlini-Bréchot, P. *et al.* Hepatitis B virus–related insertional mutagenesis occurs frequently in human liver cancers and recurrently targets human telomerase gene. *Oncogene* **22**, 3911–3916 (2003).
18. Shafritz, D.A., Shouval, D., Sherman, H.I., Hadziyannis, S.J. & Kew, M.C. Integration of hepatitis B virus DNA into the genome of liver cells in chronic liver disease and hepatocellular carcinoma. Studies in percutaneous liver biopsies and post-mortem tissue specimens. *N. Engl. J. Med.* **305**, 1067–1073 (1981).
19. Pleasance, E.D. *et al.* A comprehensive catalogue of somatic mutations from a human cancer genome. *Nature* **463**, 191–196 (2010).
20. Krzywinski, M. *et al.* Circos: an information aesthetic for comparative genomics. *Genome Res.* **19**, 1639–1645 (2009).
21. Reva, B., Antipin, Y. & Sander, C. Determinants of protein function revealed by combinatorial entropy optimization. *Genome Biol.* **8**, R232 (2007).

ONLINE METHODS

Clinical samples. The clinical and pathological features of 25 subjects and their 27 HCCs that were used for WGS are shown (**Supplementary Table 1**). HBV-related tumors were defined by the presence of HB surface antigen (HBsAg) in serum, and HCV-related tumors were defined by the presence of antibody to HCV (HCVAb) in serum. NBNC tumor was defined by a lack of both HBsAg and HCVAb. All subjects had undergone partial hepatectomy, and pathologists confirmed HCC with more than 80% viable tumor cells. High molecular weight genomic DNA was extracted from fresh-frozen tumor specimens and blood. All subjects agreed with informed consent to participate in the study following ICGC guidelines[22]. Ethical committees at RIKEN, the National Cancer Center and all groups participating in this study approved this work.

Whole-genome sequencing. We prepared insert libraries of 300–500 bp from 1.5–3 μg of genomic DNA from tumors and lymphocytes and sequenced them using the Illumina Genome Analyzer II and HiSeq 2000 platforms with paired-end reads of 50–125 bp according to the manufacturer's instructions.

Somatic point mutation and short indel calls. Read sequences were mapped by Burrows-Wheeler Aligner (BWA)[23] to the human reference genome (GRCh37). Possible PCR duplicate reads were removed by SAMtools[24] and in-house software. After filtering by pair mapping distance, mapping uniqueness and orientation between paired reads, the mapping result files were converted into the pileup format with SAMtools. Mutation calling was conducted in part on the basis of methods we have published elsewhere[1,25]. A detailed explanation is provided in the **Supplementary Note.**

Identification of significantly mutated genes. Because the number of mutations in a gene is influenced by gene length and the background mutation rate, we calculated the probability of the number of protein-altering mutations under the given mutation rate and gene length using the following set of calculations. First, we divided the genomic region into 1-Mb bins and estimated the mutation rates for point mutations and indels. Because the mutation rates in CpG sites were much higher than those of other regions (**Supplementary Fig. 3**), we estimated the mutation rate for point mutations in CpG and non-CpG sites separately. We used mutations in non-coding regions for mutation rate estimation. Second, the number of nonsynonymous sites was counted for each gene. Finally, the expected number of mutations in each gene was calculated by the total number of nonsynonymous sites and the background mutation rate. Tests of significance for each gene were performed by assuming a Poisson distribution. We adjusted for multiple testing using the Benjamini-Hochberg method[26].

Somatic genomic rearrangement calls. To identify genomic rearrangements, we used inconsistent and stretched read pairs that were uniquely mapped. We discarded read pairs with mapping quality of <30 and those with proper orientation and a distance between read pairs of <1 kb. If candidate rearrangements were supported by three or more read pairs and no rearrangement breakpoint was called within 500 bp of the tumor breakpoint in the matched lymphocyte sample, then we performed realignment to GRCh37 with blastn[27], and candidates supported by uniquely mapped read pairs were used for the validation study. We also discarded candidates that were not supported by at least one perfect-match read pair. We performed PCR validation of the candidates. Although only 10% of candidates that were supported by three read-pairs were validated, 74.1% of candidates supported by ≥4 read pairs were successfully validated (**Supplementary Fig. 11**).

Somatic copy-number alteration calling. We estimated copy-number alteration (CNA) over 5-kb windows. The ratio of standardized average depth between lymphocyte and cancer samples ($\log_2$R ratio) was calculated. CNA regions were defined by DNAcopy[28]. Segments with a $\log_2$R ratio of ≥2 or ≤−1 in two or more samples were considered as recurrent amplifications or deletions, respectively. Segments with a $\log_2$R ratio of ≥1 or ≤−0.6 in five or more samples were considered as recurrent gain (low-level amplification) and loss (low-level loss) regions, respectively.

HBV integration calls. To find HBV genome sequences in the tumor genome, we mapped read sequences to the genome of HBV genotype C (GenBank Nucleotide, NC_003977.1), which is most prevalent in Japan and east Asia. Our WGS analysis detected HBV genomic sequence in 8 out of 11 genomes of HBV-related HCCs. This is consistent with the previous observation that the HBV genomic sequence was not detected in cancerous or non-cancerous liver tissue in 20–35% of individuals with HCC that had HBsAg-positive sera[29,30]. To identify HBV integration sites, we selected read pairs in which one read was mapped to the HBV genome and the other was mapped to the human reference genome GRCh37. Twenty-three candidate sites were supported by three or more read pairs. We performed PCR validation of these candidates, and all candidates supported by three or more read pairs were successfully validated, and the breakpoints identified by Sanger sequencing were near the breakpoints predicted by the paired-end method.

PCA of the somatic substitution pattern. By comparing the genomes between the tumor and control sample from each affected subject, we counted the number of somatic mutations stratifying with substitution patterns, including C>A/G>T, C>G/G>C and C>T/G>A transversions at non-CpG sites, C>A/G>T, C>G/G>C and C>T/G>A transversions at CpG sites and T>A/A>T, T>C/A>G and T>G/A>C transversions. By dividing by the total substitution number within each individual i with HCC, we calculated substitution frequencies for these nine groups as $f_{i1}, f_{i2}, \ldots f_{i9}$, respectively. Because they are normalized so that the sum of the frequencies from all groups = 1, we used vectors of the frequencies ($\mathbf{f}_{i1}, \mathbf{f}_{i2}, \ldots \mathbf{f}_{i9}$) ($i$ = 1–27) for PCA. PCA was implemented using the R command prcomp with the scaling option on. We used principal components that had eigenvalues of >1.0. For calculating correlation coefficients between the principal-component score vectors and phenotypes of HCC (for example, HBV/HCV/NBNC classification), we used a canonical correlation analysis and tested Wilks' λ values to evaluate significance. Two HCCs (HC11 and HB11) showed quite distinct substitution patterns compared to others due to deficiency in DNA mismatch repair (**Supplementary Fig. 6a**) and were therefore excluded from PCA. PCA for other mutation sets was also performed (**Supplementary Table 14**). Also, we calculated correlation between each principal-component score and phenotypes across tumors. Similarities between the MCTs were examined by permutation test (**Supplementary Note**).

Mutation validation by exon sequencing. To discover recurrent mutations in HCCs, we amplified all protein-coding exons of the candidate genes using the DNA from 120 independent HCCs and their corresponding lymphocytes or non-cancerous livers and prepared the sequencing libraries from the amplicon mixture of pooled tumor DNA and pooled normal DNA. In total, we mixed 457 amplicons, corresponding to approximately 203 kb of DNA. The amplicon libraries were sequenced by HiSeq 2000. The average read depth per base was 174,141× and 198,103× for the tumor and non-tumor pools, respectively. We mixed in plasmid DNA as a negative control, and threshold frequencies were determined by the distribution of errors in plasmid DNA. Detailed methods have been described previously[31]. For some genes, we amplified each exon from DNA from a set of 65 HCCs and corresponding DNA from blood, and performed Sanger sequencing for each amplicon.

Digital PCR. The proportions of integration sites in cancer cell populations were examined using digital PCR[1,32]. We designed PCR primers to amplify integration sites and non-integration sites (**Supplementary Table 13**). Sequences for primers and probes are available upon request. The estimated frequencies of both integration sites (HB2-IS1 and HB2-IS2) were consistent, indicating that our estimation was highly reliable.

siRNA transfection and measurement of cell proliferation. Five HCC cell lines (JHH4, JHH5, JHH7, HuH-1 and HuH-7) were obtained from the Japanese Collection of Research Bioresources Cell Bank. Mixtures of three siRNAs targeting each gene and control, non-silencing siRNA were purchased (Thermo Fisher Scientific). Cell lines (1,000 cells) were seeded on 96-well plates and transfected with siRNA using Lipofectamine RNAiMAX (Invitrogen), according to the manufacturer's protocol. The number of cells in triplicate wells was measured by CellTiter96 AQueous One Solution Cell Proliferation Assay (Promega) on the sixth day after transfection.

22. Hudson, T.J. *et al.* International network of cancer genome projects. *Nature* 464, 993–998 (2010).

23. Li, H. & Durbin, R. Fast and accurate short read alignment with Burrows-Wheeler transform. *Bioinformatics* **25**, 1754–1760 (2009).
24. Li, H. *et al.* The Sequence Alignment/Map format and SAMtools. *Bioinformatics* **25**, 2078–2079 (2009).
25. Fujimoto, A. *et al.* Whole-genome sequencing and comprehensive variant analysis of a Japanese individual using massively parallel sequencing. *Nat. Genet.* **42**, 931–936 (2010).
26. Benjamini, Y. & Hochberg, Y. Controlling the false discovery rate: a practical and powerful approach to multiple testing. *J. R. Stat. Soc. B* **57**, 289–300 (1995).
27. Altschul, S.F., Gish, W., Miller, W., Myers, E.W. & Lipman, D.J. Basic local alignment search tool. *J. Mol. Biol.* **215**, 403–410 (1990).
28. Andersson, R. *et al.* A segmental maximum a posteriori approach to genome-wide copy number profiling. *Bioinformatics* **24**, 751–758 (2008).
29. Zhou, Y.Z., Butel, J.S., Li, P.J., Finegold, M.J. & Melnick, J.L. Integrated state of subgenomic fragments of hepatitis B virus DNA in hepatocellular carcinoma from mainland China. *J. Natl. Cancer Inst.* **79**, 223–231 (1987).
30. Gozuacik, D. *et al.* Identification of human cancer-related genes by naturally occurring Hepatitis B Virus DNA tagging. *Oncogene* **20**, 6233–6240 (2001).
31. Puente, X.S. *et al.* Whole-genome sequencing identifies recurrent mutations in chronic lymphocytic leukaemia. *Nature* **475**, 101–105 (2011).
32. Qin, J., Jones, R.C. & Ramakrishnan, R. Studying copy number variations using a nanofluidic platform. *Nucleic Acids Res.* **36**, e116 (2008).

doi:10.1038/ng.2291

Original Paper

Neuro
-endocrinology

Neuroendocrinology 2012;96:324–332
DOI: 10.1159/000338794

Received: December 19, 2011
Accepted after revision: April 9, 2012
Published online: August 28, 2012

Comparison of Chemotherapeutic Treatment Outcomes of Advanced Extrapulmonary Neuroendocrine Carcinomas and Advanced Small-Cell Lung Carcinoma

T. Terashima[a, f] C. Morizane[a] N. Hiraoka[e] H. Tsuda[b] T. Tamura[c] Y. Shimada[d]
S. Kaneko[f] R. Kushima[b] H. Ueno[a] S. Kondo[a] M. Ikeda[g] T. Okusaka[a]

[a]Hepatobiliary and Pancreatic Oncology Division, [b]Pathology Division, [c]Internal Medicine and Thoracic Oncology Division, and [d]Gastrointestinal Oncology Division, National Cancer Center Hospital, and [e]Pathology Division, National Cancer Center Research Institute, Tokyo, [f]Gastroenterology, Kanazawa University Hospital, Kanazawa, and [g]Division of Hepatobiliary and Pancreatic Oncology, National Cancer Center Hospital East, Kashiwa, Japan

Key Words
Extrapulmonary neuroendocrine carcinoma · Small-cell lung carcinoma · Chemotherapy · Prognosis · Prognostic factor

Abstract
Background: The chemotherapy for small-cell lung carcinoma (SCLC) has been adopted for advanced extrapulmonary neuroendocrine carcinomas (EP-NECs). The aim of this study was to clarify the efficacy of standard SCLC regimens when used to treat EP-NECs and to compare the outcome with that for SCLC. ***Methods:*** We reviewed the medical records of 136 patients (41 with EP-NEC and 95 with SCLC) who were treated using a platinum-containing regimen for advanced disease between January 2000 and October 2008 at our hospital. ***Results:*** The primary site of the EP-NEC was the gastrointestinal tract in 18 patients (GI tract group); the liver, biliary tract or pancreas in 16 patients (HBP group), and other sites in 7 patients ('others' group). The response rate in the SCLC patients was 77.8%, and the response rate in the EP-NEC patients was 30.8% (37.5% in the GI tract group, 12.5% in the HBP group, and 57.1% in the 'others' group). The median survival time for the SCLC patients was 13.6 months, while that for the EP-NEC patients was 9.2 months (14.9 months in the GI tract group, 7.8 months in the HBP group, and 8.9 months in the 'others' group). A multivariate analysis demonstrated that a poor performance status, liver involvement, and the treatment regimen were independent unfavorable prognostic factors. ***Conclusion:*** The response rate and prognosis of the patients with advanced EP-NECs were worse than those of the patients with SCLC in this study. The Eastern Cooperative Oncology Group performance status, liver involvement, and treatment regimen had a larger impact on the prognosis than the primary tumor site, as demonstrated by multivariate analysis.

Introduction

Neuroendocrine neoplasms are defined as all neoplasms originating from endocrine glands, nerve elements, or from elements of the diffuse neuroendocrine system [1]. The World Health Organization (WHO) has proposed a grading system for neuroendocrine neo-

KARGER

Fax +41 61 306 12 34
E-Mail karger@karger.ch
www.karger.com

0028–3835/12/0964–0324$38.00/0

Accessible online at:
www.karger.com/nen

Chigusa Morizane, MD
Hepatobiliary and Pancreatic Oncology Division
National Cancer Center Hospital
5-1-1 Tsukiji, Chuo-ku, Tokyo 104-0045 (Japan)
Tel. +81 3 3542 2511, E-Mail cmorizan@ncc.go.jp

plasms that divides them into three tiers based on proliferation as follows [2]: (1) neuroendocrine tumor (NET) (G1): mitotic count <2 per 10 high power fields (HPF) and/or a Ki67 index of ≤2%; (2) NET (G2): mitotic count 2–20 per 10 HPF and/or a Ki67 index of 3–20%, and (3) neuroendocrine carcinoma (NEC): mitotic count >20 per 10 HPF and/or a Ki67 index of >20%. Among these classes, NEC is a poorly differentiated, high-grade malignant neoplasm. The definition of NEC refers to neoplasms previously classified as small-cell carcinoma or poorly differentiated (neuro)endocrine carcinoma (PDNEC). Since the first report of 'extrapulmonary oat cell carcinoma' of the mediastinum by Duguid and Kennedy [3] in 1930, extrapulmonary NECs (EP-NECs) have been reported to arise in a variety of organs, such as the gastrointestinal tract, pancreas, head and neck region, or urogenital tract [4–16]. EP-NECs are a fairly rare, heterogeneous disease entity, and no standard treatment has been established [17, 18]. Especially for extended or recurrent EP-NECs, treatment with combined etoposide and cisplatin, which is a representative regimen for the treatment of small-cell lung carcinoma (SCLC), has been mainly adopted [19–21] until now because these tumors share many features, including their immunohistochemical findings and aggressive clinical behavior [8]. However, some cytogenetic analyses have revealed differences between the two entities [6, 14, 22]. Therefore, EP-NECs may differ from SCLC with respect to their sensitivity to anticancer agents or patient outcome [7]. The aim of the present study was to clarify the efficacy of standard SCLC regimens when used for the treatment of advanced EP-NECs and to compare the outcome with that for SCLC. Moreover, we compared the sensitivity to systemic chemotherapy and the patient outcome according to the primary tumor site to identify prognostic factors.

Materials and Methods

Patients and Methods

This study was approved by the Ethics Committee of the National Cancer Center, Japan. The pathology records of the National Cancer Center Hospital, Tokyo, Japan (January 2000 to December 2008) were searched for neuroendocrine neoplasms. In all the patients, a fine-needle biopsy or surgical specimen had been used for the pathological diagnosis. Clinical information was obtained from the patients' medical records. Patients with EP-NEC or small-cell lung cancer according to the WHO classification [2, 23], chemotherapy-naïve patients with extended or recurrent disease, and patients treated with platinum-based combined chemotherapy [a regimen consisting of cisplatin and etoposide (PE regimen), cisplatin and irinotecan (IP regimen), or carboplatin and etoposide (CE regimen)] were considered for enrollment. If accurate proliferation fraction, such as Ki67 index or mitotic count, could not be obtained, tumor differentiation was diagnosed morphologically. In such cases, PDNECs according to the WHO 2004 [24] classification were considered as eligible. Patients who were participating in ongoing prospective clinical trials were excluded from the analysis. All the patients underwent computed tomography (CT) examinations to determine the tumor stage. CT scans of the brain or bone scans were also performed mainly in symptomatic patients. Upper and lower gastrointestinal endoscopic examinations were performed in patients with gastrointestinal NECs or unknown primary tumors. An extended NEC stage was defined as the presence of any single or multiple metastases at any distant anatomical site (including non-regional nodes), corresponding to the extended stage of the two-stage system for SCLC that was originally introduced by the Veterans' Administration Lung Study Group [25]. We investigated the patients' backgrounds, treatment efficacy, and the patient outcome according to the primary site. Thereafter, we compared the sensitivity to systemic chemotherapy and the patient outcome according to the primary tumor site to identify prognostic factors.

Study Design

The response to chemotherapy was assessed according to the Response Evaluation Criteria in Solid Tumors (RECIST), version 1.0 [26]. A response rate was defined as the sum of the complete response rate and the partial response rate. The χ^2 test was used to assess differences in the patient characteristics of the EP-NEC and SCLC groups and the relation between the primary tumor site and the response rate. Overall survival (OS) was calculated from the first day of treatment until the date of death or the last day of the follow-up period. In the univariate analysis, the cumulative survival proportions were calculated using the Kaplan-Meier method [27], and any differences were evaluated using the log-rank test. Only variables that achieved statistical significance in the univariate analysis were subsequently evaluated in the multivariate analysis using Cox's proportional hazards regression model [28]. A p value of <0.05 was considered statistically significant, and all the tests were two-sided. All statistical analyses were performed using the SPSS statistical software program package (SPSS version 11.0 for Windows).

Results

We retrospectively reviewed 981 patients with a pathologically confirmed diagnosis of neuroendocrine neoplasms (511 from extrapulmonary organs and 470 from the lung). Overall, 136 patients (41 with EP-NECs and 95 with SCLC) met the above-described criteria (fig. 1). The patient characteristics are summarized in table 1. The median age of the patients with EP-NECs was 58 years, which was significantly younger than that of the patients with SCLC (67 years). The patients included 26 males (63.4%) with EP-NECs and 75 males (78.9%) with SCLC; while the percentage of male subjects with EP-NECs was

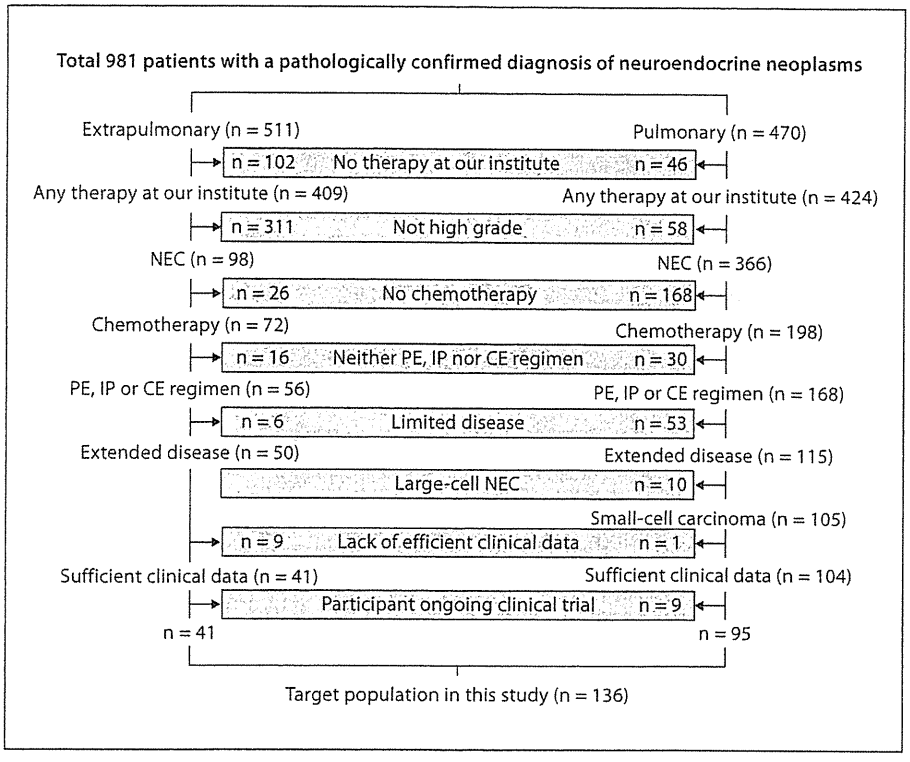

Fig. 1. Study population. The target population of this study was patients with extended or recurrent extrapulmonary PDNECs or small-cell carcinoma who had been treated with chemotherapy (PE, IP or CE regimen) at our institute.

lower than that of male subjects with SCLC, the difference was not statistically significant. The majority of patients in both groups had a good performance status: 97.6% of the patients with EP-NECs and 90.5% of the patients with SCLC had an Eastern Cooperative Oncology Group performance status (ECOG PS) of 0 or 1. Brain and lymph node metastases were observed more frequently among patients with SCLC than among those with EP-NECs ($p < 0.01$ and $p < 0.01$, respectively), whereas liver involvement was observed significantly more often among patients with EP-NECs than among those with SCLC ($p < 0.01$). The major primary sites of EP-NECs were the stomach in 10 patients, followed by the pancreas in 9 patients and the esophagus in 8 patients (table 2). We divided the patients with EP-NECs into three groups according to the primary tumor sites: the gastrointestinal tract group (GI tract group), comprising 43.9% of the EP-NECs; the liver, biliary tract or pancreas group (HBP group), comprising 39.0% of the EP-NECs, and the 'others' group (prostate, thymus, bladder, and unknown primary), comprising 17.1% of the EP-NECs. Patient characteristics are summarized in table 1. Overall, systemic chemotherapy was performed according to the PE regimen in 31 patients, the IP regimen in 70 patients, and the CE regimen in 35 patients (table 3). The tumor responses to chemotherapy are shown in table 4. The response rate was significantly higher in the SCLC group (77.8%) than in the EP-NEC group (30.8%; $p < 0.01$). Of the patients with EP-NECs, the response rate in the HBP group (12.5%) was significantly lower than that of the 'others' group (57.1%; $p = 0.025$) and tended to be lower than that in the GI group (37.5%; $p = 0.10$). The median survival time (MST) of the patients with EP-NECs was 9.2 months and had a tendency to be worse than that of SCLC patients with 13.6 months, but the difference was not significant ($p = 0.067$; fig. 2). The 1-year survival rate (61.1 vs. 38.6%) was better for the patients with SCLC than EP-NECs. And a few patients (11.8%) with SCLC but no patients with EP-NECs survived longer than 3 years. The MSTs of patients treated with an IP regimen, PE regimen, and CE regimen are shown in table 5. Of the patients with EP-NECs, the MSTs of the patients in the GI tract group, the HBP group, and the 'others' group were 14.9, 7.8, and 8.9 months, respectively ($p < 0.01$; fig. 3). The following 8 of the 15 pretreatment variables that were evaluated were identified as being significantly associated with the survival time in univariate analyses (table 6): ECOG PS ($p < 0.01$), primary site ($p < 0.01$), neuron-specific enolase (NSE; $p = 0.025$), hemoglobin ($p = 0.029$), albumin ($p < 0.01$), alkaline phosphatase ($p = 0.030$), liv-

Table 1. Clinical characteristics of the patients

	EP-NECs				SCLC	p value
	Total	GI tract group	HBP group	'Others' group		
Patients	41	18	16	7	95	
Age, years						<0.01*
Median	58	63.5	46.5	59	67	
Range	27–79	27–79	30–69	33–84	43–84	
Gender, n (%)						0.057**
Male	26 (63)	15 (83)	8 (50)	3 (43)	75 (79)	
Female	15 (37)	3 (17)	8 (50)	4 (57)	20 (21)	
EGOG PS, n (%)						0.28**
0	12 (29)	4 (22)	4 (25)	4 (57)	21 (21)	
1	28 (68)	14 (78)	11 (69)	3 (43)	65 (68)	
2	1 (2)	0	1 (6)	0	9 (9)	
NSE, ng/ml						0.050*
Median	43.8	34.2	127.7	14.6	57.2	
Range	7.5–1,930	9.2–210.5	20.7–1930	7.5–571.0	5.5–1,158	
ProGRP, pg/ml						0.69*
Median	43.0	47.9	31.3	48.9	668.4	
Range	5.3–63,090	5.3–13,810	11.9–63,090	21.2–117.1	18.3–40,550	
Metastatic site, n (%)						
Liver	30 (73)	14 (78)	13 (81)	3 (43)	21 (22)	<0.01**
Brain	2 (5)	1 (6)	0	1 (14)	27 (28)	<0.01**
Bone	4 (10)	1 (6)	1 (6)	2 (29)	22 (23)	0.068**
Lung	5 (12)	1 (6)	3 (19)	1 (14)	–	–
Lymph node	21 (51)	13 (72)	5 (31)	0	76 (80)	<0.01**

ProGRP = Pro-gastrin-releasing peptide. * Student's t test, ** χ^2 test.

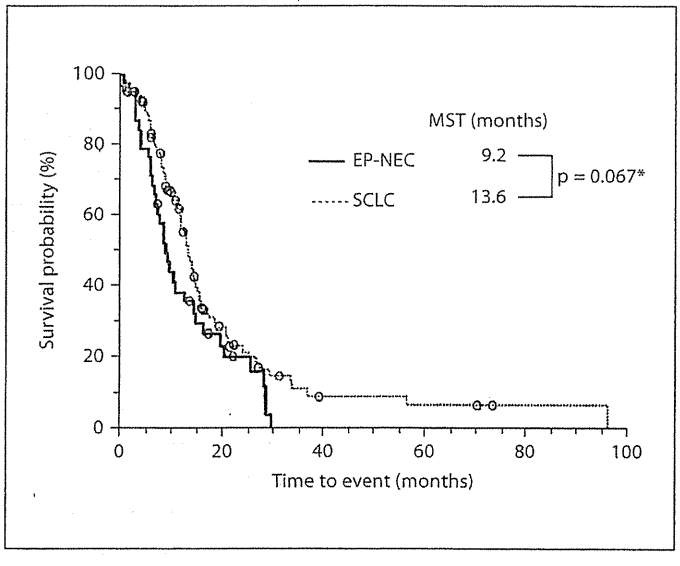

Fig. 2. Kaplan-Meier plot of OS. The MST of the patients with EP-NECs was 9.2 months and had a tendency to be shorter than that of patients with SCLC, which was 13.6 months. * log-rank test.

Table 2. Primary tumor site of the patients with EP-NECs

GI tract group	
Stomach	10
Esophagus	8
HBP group	
Pancreas	9
Gallbladder	4
Liver	3
'Others' group	
Thymus	2
Prostate	2
Bladder	2
CUP	2

CUP = Carcinoma of unknown primary site.

Table 3. Chemotherapy regimens

	EP-NECs				SCLC	Total
	Total	GI tract	HBP	Others		
CDDP + VP-16	18	1	16	1	13	31
CDDP + CPT-11	22	17	0	5	48	70
CBDCA + VP-16	1	0	0	1	34	35
Total	41	18	16	7	104	136

CDDP = Cisplatin; VP-16 = etoposide; CPT-11 = irinotecan; CBDCA = carboplatin.

Table 4. Tumor responses

	EP-NECs				SCLC
	Total	GI tract	HBP	Others	
Complete response	1	0	0	1	5
Partial response	11	6	2	3	72
Stable disease	17	6	9	2	7
Progressive disease	10	4	5	1	48
Not evaluable	2	2	0	0	6
Response rate	30.8%	37.5%	12.5%	57.1%	77.8%
			$p = 0.10^*$	$p = 0.025^*$	
			$p < 0.01^*$		(RECIST version 1.0)

* χ^2 test.

Table 5. The MSTs of the patients treated with IP regimen, PE regimen, and CE regimen

	EP-NECs			SCLC			Total		
	n	MST		n	MST		n	MST	
CDDP + VP-16	18	7.3	$p = 0.001^*$	13	12.4	$p = 0.023^*$	31	8.9	$p < 0.001^*$
CDDP + CPT-11	22	14.9		48	16.6		70	16.6	
CBDCA + VP-16	1	16.9		34	9.3	$p = 0.023^*$	35	9.3	$p = 0.038^*$

CDDP = Cisplatin; VP-16 = etoposide; CPT-11 = irinotecan; CBDCA = carboplatin. * log-rank test.

Table 6. Prognostic factors (univariate analysis)

	n	Median OS ± SE months	p*
Age			
≥64 years	66	12.5 ± 0.97	0.66
<64 years	70	12.9 ± 2.07	
Sex			
Male	101	12.4 ± 0.99	0.74
Female	35	12.9 ± 1.34	
ECOG PS			
0–1	126	13.5 ± 1.64	<0.01
2–3	10	5.1 ± 3.02	
Primary site			
Lung	95	13.6 ± 0.33	<0.01
GI tract	18	14.9 ± 8.03	
HBP	16	7.8 ± 1.49	
Others	7	8.9 ± 3.52	
NSE			
≥15 ng/ml	118	12.1 ± 1.55	0.025
<15 ng/ml	18	26.2 ± 5.05	
ProGRP			
≥45 pg/ml	97	13.3 ± 1.35	0.83
<45 pg/ml	39	12.4 ± 1.42	
Hb			
≥12 g/dl	85	13.7 ± 0.40	0.029
<12 g/dl	51	10.3 ± 1.96	
CRP			
≥0.4 mg/dl	89	11.3 ± 1.69	0.056
<0.4 mg/dl	47	14.9 ± 1.82	
Alb			
≥3.7 g/dl	72	14.6 ± 1.40	<0.01
<3.7 g/dl	64	9.3 ± 0.43	
ALP			
≥360 IU/l	37	9.2 ± 0.68	0.030
<360 IU/l	99	13.8 ± 0.88	
LDH			
≥230 IU/l	103	11.6 ± 1.86	0.058
<230 IU/l	33	18.0 ± 5.54	
Brain metastases			
Presence	29	12.4 ± 0.55	0.66
Absence	107	13.6 ± 0.97	
Bone metastases			
Presence	26	10.4 ± 3.72	0.078
Absence	110	13.6 ± 0.36	
Liver metastases			
Presence	51	9.1 ± 0.35	<0.01
Absence	85	14.1 ± 1.46	
Regimen			
CDDP + VP-16	31	8.9 ± 0.66	<0.01
CBDCA + VP-16	35	9.3 ± 1.45	
CDDP + CPT-11	70	16.6 ± 4.38	

ProGRP = Pro-gastrin-releasing peptide; Hb = hemoglobin; CRP = C-reactive peptide; Alb = albumin; ALP = alkaline phosphatase; LDH = lactate dehydrogenase; CDDP = cisplatin; VP-16 = etoposide; CBDCA = carboplatin; CPT-11 = irinotecan. * log-rank test.

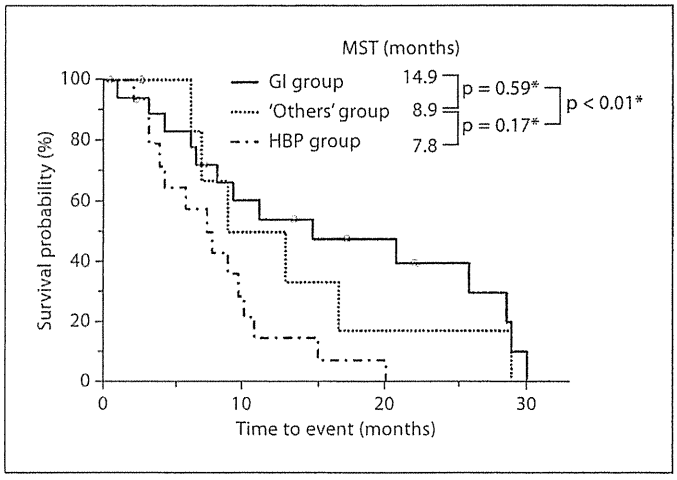

Fig. 3. Kaplan-Meier curves of OS of the patients with EP-NECs. The MSTs of the patients in the GI tract group, the HBP group, and the 'others' group were 14.9, 7.8, and 8.9 months, respectively. The HBP group had the worst prognosis. * log-rank test.

er involvement ($p < 0.01$), and chemotherapy regimen ($p < 0.01$). Only 3 of the above factors were identified as independent unfavorable prognostic factors in a multivariate Cox regression model: an ECOG PS of 2 or 3 (hazard ratio 3.786; $p < 0.01$), liver involvement (hazard ratio 1.943; $p = 0.013$), and the PE regimen (hazard ratio compared with the IP regimen 1.990; $p = 0.032$; table 7).

Discussion

The definition of NET has been confused for a long time, and the clinical and pathologic features of NETs have been described by many investigators, with most studies focusing on subsets of tumors restricted to one organ or organ system. Site-longitudinal grading, staging, and classification systems have been developed by the WHO [2, 23] and the European Neuroendocrine Tumor Society (ENETS) [29, 30]. Among the parameters of those classification systems, the proliferative index has emerged as a fundamental grading characteristic that now appears in most major schemata. Within these schemata, NECs represent the highest grade of malignancy, and patients with these tumor types have the worst outcome among all patients with neuroendocrine neoplasms [31, 32]. Therefore, the development of an effective therapy for this disease entity is essential.

Systemic chemotherapy for patients with EP-NECs has been conducted according to the regimens used for

Table 7. Prognostic factors (multivariate analysis)

	Hazard ratio (95% CI)	p*
ECOG PS		
2–3	3.786 (1.736–8.259)	<0.01
Primary site		
Lung		
GI tract	1.061 (0.531–2.121)	0.87
HBP	1.390 (0.593–3.255)	0.45
Others	1.364 (0.534–3.480)	0.52
NSE		
≥15 ng/ml	1.480 (0.782–2.803)	0.23
Hb		
<12 g/dl	1.144 (0.740–1.768)	0.55
Alb		
<3.7 g/dl	1.381 (0.890–2.144)	0.15
ALP		
<360 IU/l	1.189 (0.682–2.075)	0.54
Liver involvement		
Presence	1.943 (1.146–3.295)	0.014
Regimen		
CDDP + CPT-11		
CDDP + VP-16	1.990 (1.062–3.731)	0.032
CBDCA + VP-16	1.487 (0.873–2.532)	0.14

Hb = Hemoglobin; Alb = albumin; ALP = alkaline phosphatase; CDDP = cisplatin; CPT-11 = irinotecan; VP-16 = etoposide; CBDCA = carboplatin. * Cox proportional hazards model.

SCLC; however, little is known about treatment efficacy because of the rareness of these cases, unlike SCLC (which accounts for about 20% of all lung cancers). Consequently, we decided to conduct the present investigation. In an attempt to unify the therapeutic procedures among unified patients, the candidates for enrollment were rigidly restricted to patients with pathologically confirmed EP-NECs and SCLC, extended or recurrent disease, and who had been treated with the PE, IP, or CE regimen. The PE or IP regimens are presently considered to be the standard treatment regimens for patients with extended SCLC [33–35]. The CE regimen has been reported to have a similar efficacy to the PE regimen among patients with SCLC and can be considered as an alternative treatment regimen [36].

The first aim of this study was to clarify the efficacy of standard SCLC regimens when used to treat advanced EP-NECs and to compare the treatment outcome with that for SCLC. Our study showed that the response rate of the patients with EP-NECs was lower than that of the patients with SCLC. The objective response rate to platinum-based chemotherapy was 77.8% for the patients with SCLC, and the MST in the present study was 13.6 months, which was similar to previously reported survival times [33, 34, 36]. On the other hand, the efficacy of such regimens against EP-NECs seemed to be worse in the present study, with a response rate of 31.7% compared with 33–66.7% in previous reports [5, 7, 10, 20, 21]. Although the reason for the difference in the treatment efficacies was unknown, possible reasons include the differences in the criteria used to evaluate response and the relatively small number of patients. Additionally, the response rates of EP-NECs with different primary sites were significantly different, with the HBP group showing the lowest response rate. This finding also disagreed with Brenner et al.'s [5] report, which showed no differences in the response to chemotherapy among the different anatomical locations. The patients with EP-NECs tended to have unfavorable outcomes compared with the patients with SCLC in our study. Some reports have shown that the OS of patients with EP-NECs was better than that of patients with SCLC [7, 16]. In the present study, the most common primary sites of the EP-NECs were the stomach, pancreas, and esophagus. On the other hand, relatively few patients had tumors arising in the reproductive tract, breast, or head and neck region, which have been reported to be associated with a better prognosis [4, 9–12]. At our institution, genitourinary EP-NECs tend to be resected, and head and neck EP-NECs are often treated using chemoradiotherapy. In other words, the outcomes of the patients in a particular study might depend on the ratio of the primary sites. Moreover, an interesting finding in the present study was that although liver involvement was identified as a prognostic factor in a multivariate analysis, the primary site was not a prognostic factor. In fact, liver metastasis is a well-documented poor prognostic factor in patients with NETs [22, 37–40]. Actually, 73% of the EP-NECs exhibited liver involvement in the present study, whereas only 22% of the SCLCs exhibited liver involvement.

Another interesting point of the present study is that the IP regimen was associated with a significantly more favorable outcome than the PE regimen in the multivariate analysis. When the outcome of the SCLC patients was examined according to the chemotherapeutic regimen that was used, the MST associated with the IP regimen was 16.6 months, which was significantly longer than that associated with the PE regimen (12.4 months) or the CE regimen (9.3 months) ($p = 0.023$ and $p = 0.023$, respectively; table 5). These results agree with those of a Japanese report by Noda et al. [35]. A similar trend was observed among patients with EP-NECs in our study.

However, this result should be interpreted with caution because of the bias introduced by the different treatment policies with regard to the selection of chemotherapeutic regimens among the divisions of our institute. For example, all the patients in the HBP group were treated using the PE regimen, whereas a large proportion of the patients in the GI and 'others' groups were treated using the IP regimen (table 3).

The objectives of this study included not only patients with 'extrapulmonary small-cell carcinoma' but also those with 'EP-NEC diagnosed based on a high Ki67 index or high mitotic count without small-cell morphological features; NEC other than small-cell carcinoma'. It is possible that 'NEC other than small-cell carcinoma' may be biologically and clinically different from small-cell carcinoma, and these differences could influence the treatment outcomes of NEC in this study. However, although the terms 'small-cell carcinoma' and 'large-cell carcinoma' were specified in the WHO 2010 classification, no definite indicators distinguishing 'NEC other than small-cell carcinoma' from 'small-cell carcinoma' exist. Therefore, we refrained from comparing them in this study. Additionally, some prognostic factors, such as the Ki67 index, mitotic count or degree of necrosis, may also influence the treatment outcomes. Because information regarding these factors could not be obtained for all the patients in this study and because our main purpose in this study was to compare the clinical outcomes according to the primary tumor site, we did not evaluate the chemosensitivity or the patient outcome according to these factors. Nevertheless, these points are very important clinical questions and should be examined in future studies.

Another limitation of this study was its retrospective nature, and a prospective trial with a large number of patients treated using the same chemotherapeutic regimen is needed to confirm our findings.

In conclusion, the response rate and prognosis of patients with extended or recurrent EP-NECs, especially those originating in the liver, biliary tract, or pancreas, were worse than those of the patients with SCLC in this study. The ECOG PS, liver involvement, and treatment regimen had a larger impact on the prognosis than the primary tumor site, as demonstrated by multivariate analysis.

Acknowledgement

The authors thank Ikuo Sekine (Internal Medicine and Thoracic Oncology Division, National Cancer research Institute) for the amendment of clinical information of the patients with SCLC.

Disclosure Statement

The authors have no conflicts of interest.

References

1 Barakat MT, Meeran K, Bloom SR: Neuroendocrine tumours. Endocr Relat Cancer 2004; 11:1–18.

2 Rindi G, Arnold R, Bosman FT, et al: Nomenclature and classification of neuroendocrine neoplasms of the digestive system. WHO classification of tumours of the digestive system. Lyon, IARC Press, 2010.

3 Duguid J, Kennedy A: Oat-cell tumors of mediastinal glands. J Pathol Bacteriol 1930;33: 93–99.

4 Brennan SM, Gregory DL, Stillie A, Herschtal A, Mac Manus M, Ball DL: Should extrapulmonary small cell cancer be managed like small cell lung cancer? Cancer 2010;116: 888–895.

5 Brenner B, Shah MA, Gonen M, Klimstra DS, Shia J, Kelsen DP: Small-cell carcinoma of the gastrointestinal tract: a retrospective study of 64 cases. Br J Cancer 2004;90:1720–1726.

6 Brenner B, Tang LH, Klimstra DS, Kelsen DP: Small-cell carcinomas of the gastrointestinal tract: a review. J Clin Oncol 2004;22: 2730–2739.

7 Cicin I, Karagol H, Uzunoglu S, Uygun K, Usta U, Kocak Z, et al: Extrapulmonary small-cell carcinoma compared with small-cell lung carcinoma: a retrospective single-center study. Cancer 2007;110:1068–1076.

8 Galanis E, Frytak S, Lloyd RV: Extrapulmonary small cell carcinoma. Cancer 1997;79: 1729–1736.

9 Haider K, Shahid RK, Finch D, Sami A, Ahmad I, Yadav S, et al: Extrapulmonary small cell cancer: a Canadian province's experience. Cancer 2006;107:2262–2269.

10 Kim JH, Lee SH, Park J, Kim HY, Lee SI, Nam EM, et al: Extrapulmonary small-cell carcinoma: a single-institution experience. Jpn J Clin Oncol 2004;34:250–254.

11 Lee SS, Lee JL, Ryu MH, Chang HM, Kim TW, Kim WK, et al: Extrapulmonary small cell carcinoma: single center experience with 61 patients. Acta Oncol 2007;46:846–851.

12 Lin YL, Chung CY, Chang CS, Wu JS, Kuo KT, Kuo SH, et al: Prognostic factors in extrapulmonary small cell carcinomas. A large retrospective study. Oncology 2007;72:181–187.

13 Moskal TL, Zhang PJ, Nava HR: Small cell carcinoma of the gallbladder. J Surg Oncol 1999;70:54–59.

14 Takubo K, Nakamura K, Sawabe M, Arai T, Esaki Y, Miyashita M, et al: Primary undifferentiated small cell carcinoma of the esophagus. Hum Pathol 1999;30:216–221.

15 Walenkamp AM, Sonke GS, Sleijfer DT: Clinical and therapeutic aspects of extrapulmonary small cell carcinoma. Cancer Treat Rev 2009;35:228–236.

16 Wong YN, Jack RH, Mak V, Henrik M, Davies EA: The epidemiology and survival of extrapulmonary small cell carcinoma in South East England, 1970–2004. BMC Cancer 2009;9:209.
17 Ahlman H, Nilsson O, McNicol AM, Ruszniewski P, Niederle B, Ricke J, et al: Poorly-differentiated endocrine carcinomas of midgut and hindgut origin. Neuroendocrinology 2008;87:40–46.
18 Nilsson O, Van Cutsem E, Delle Fave G, Yao JC, Pavel ME, McNicol AM, et al: Poorly differentiated carcinomas of the foregut (gastric, duodenal and pancreatic). Neuroendocrinology 2006;84:212–215.
19 Fjallskog ML, Granberg DP, Welin SL, Eriksson C, Oberg KE, Janson ET, et al: Treatment with cisplatin and etoposide in patients with neuroendocrine tumors. Cancer 2001;92:1101–1107.
20 Mitry E, Baudin E, Ducreux M, Sabourin JC, Rufie P, Aparicio T, et al: Treatment of poorly differentiated neuroendocrine tumours with etoposide and cisplatin. Br J Cancer 1999;81:1351–1355.
21 Moertel CG, Kvols LK, O'Connell MJ, Rubin J: Treatment of neuroendocrine carcinomas with combined etoposide and cisplatin. Evidence of major therapeutic activity in the anaplastic variants of these neoplasms. Cancer 1991;68:227–232.
22 Janson ET, Holmberg L, Stridsberg M, Eriksson B, Theodorsson E, Wilander E, et al: Carcinoid tumors: analysis of prognostic factors and survival in 301 patients from a referral center. Ann Oncol 1997;8:685–690.
23 Travis WD, Brambilla E, Müller-Hermelink HK, Harris CC; WHO, IARC (eds): World Health Organization Classification of Tumours. Pathology and Genetics of Tumours of the Lung, Pleura, Thymus and Heart. Lyon, IARC Press, 2004.
24 DeLellis RA; WHO, IARC (eds): World Health Organization Classification of Tumours. Pathology and Genetics of Tumours of Endocrine Organs. Lyon, IARC Press, 2004.
25 Zelen M: Keynote address on biostatistics and data retrieval. Cancer Chemother Rep 3 1973;4:31–42.
26 Therasse P, Arbuck SG, Eisenhauer EA, Wanders J, Kaplan RS, Rubinstein L, et al: New guidelines to evaluate the response to treatment in solid tumors. European Organization for Research and Treatment of Cancer, National Cancer Institute of the United States, National Cancer Institute of Canada. J Natl Cancer Inst 2000;92:205–216.
27 Kaplan E, Meier P: Nonparametric estimation from incomplete observation. J Am Stat Assoc 1958;53:457–481.
28 Cox D: Regression models and life-tables. J R Stat Soc B 1972;34:187–200.
29 Rindi G, Kloppel G, Alhman H, Caplin M, Couvelard A, de Herder WW, et al: TNM staging of foregut (neuro)endocrine tumors: a consensus proposal including a grading system. Virchows Arch 2006;449:395–401.
30 Rindi G, Kloppel G, Couvelard A, Komminoth P, Korner M, Lopes JM, et al: TNM staging of midgut and hindgut (neuro)endocrine tumors: a consensus proposal including a grading system. Virchows Arch 2007;451:757–762.
31 Kloppel G. Tumour biology and histopathology of neuroendocrine tumours. Best Pract Res Clin Endocrinol Metab 2007;21:15–31.
32 Yao JC, Hassan M, Phan A, Dagohoy C, Leary C, Mares JE, et al: One hundred years after 'carcinoid': epidemiology of and prognostic factors for neuroendocrine tumors in 35,825 cases in the United States. J Clin Oncol 2008;26:3063–3072.
33 Fukuoka M, Furuse K, Saijo N, Nishiwaki Y, Ikegami H, Tamura T, et al: Randomized trial of cyclophosphamide, doxorubicin, and vincristine versus cisplatin and etoposide versus alternation of these regimens in small-cell lung cancer. J Natl Cancer Inst 1991;83:855–861.
34 Hanna N, Bunn PA Jr, Langer C, Einhorn L, Guthrie T Jr, Beck T, et al: Randomized phase III trial comparing irinotecan/cisplatin with etoposide/cisplatin in patients with previously untreated extensive-stage disease small-cell lung cancer. J Clin Oncol 2006;24:2038–2043.
35 Noda K, Nishiwaki Y, Kawahara M, Negoro S, Sugiura T, Yokoyama A, et al: Irinotecan plus cisplatin compared with etoposide plus cisplatin for extensive small-cell lung cancer. N Engl J Med 2002;346:85–91.
36 Okamoto H, Watanabe K, Kunikane H, Yokoyama A, Kudoh S, Asakawa T, et al: Randomised phase III trial of carboplatin plus etoposide vs split doses of cisplatin plus etoposide in elderly or poor-risk patients with extensive disease small-cell lung cancer: JCOG 9702. Br J Cancer 2007;97:162–169.
37 Bettini R, Boninsegna L, Mantovani W, Capelli P, Bassi C, Pederzoli P, et al: Prognostic factors at diagnosis and value of WHO classification in a mono-institutional series of 180 non-functioning pancreatic endocrine tumours. Ann Oncol 2008;19:903–908.
38 Kouvaraki MA, Ajani JA, Hoff P, Wolff R, Evans DB, Lozano R, et al: Fluorouracil, doxorubicin, and streptozocin in the treatment of patients with locally advanced and metastatic pancreatic endocrine carcinomas. J Clin Oncol 2004;22:4762–4771.
39 Madeira I, Terris B, Voss M, Denys A, Sauvanet A, Flejou JF, et al: Prognostic factors in patients with endocrine tumours of the duodenopancreatic area. Gut 1998;43:422–427.
40 Panzuto F, Nasoni S, Falconi M, Corleto VD, Capurso G, Cassetta S, et al: Prognostic factors and survival in endocrine tumor patients: comparison between gastrointestinal and pancreatic localization. Endocr Relat Cancer 2005;12:1083–1092.